Towards on-line treatment verification using *cine* EPID for hypofractionated lung radiotherapy

Xiaoli Tang[1], Tong Lin[1, 2], and Steve Jiang[1]
[1]*Department of Radiation Oncology, University of California San Diego, La Jolla, CA 92093, USA*
[2] *Key Laboratory of Machine Perception (Ministry of Education), School of EECS, Peking University, Beijing 100871, China*
sbjiang@ucsd.edu

Abstract

We propose a novel approach for on-line treatment verification using cine EPID (Electronic Portal Imaging Device) images for hypofractionated lung radiotherapy based on a machine learning algorithm. Hypofractionated lung radiotherapy has high precision requirement, and it is essential to effectively monitor the target making sure the tumor is within beam aperture. We model the treatment verification problem as a two-class classification problem and apply Artificial Neural Network (ANN) to classify the cine EPID images acquired during the treatment into corresponding classes—tumor inside or outside of the beam aperture. Training samples of ANN are generated using digitally reconstructed radiograph (DRR) with artificially added shifts in tumor location—to simulate cine EPID images with different tumor locations. Principal Component Analysis (PCA) is used to reduce the dimensionality of the training samples and cine EPID images acquired during the treatment. The proposed treatment verification algorithm has been tested on six hypofrationated lung patients in a retrospective fashion. On average, our proposed algorithm achieved 94.66% classification accuracy, 94.50% recall rate, and 99.79% precision rate.

1. Introduction

In the United States, lung cancer is the second most prevalent cancer and the leading cause of cancer death, accounting for about 30% of all cancer mortality [1]. Hypofractionated lung radiotherapy is being increasingly employed as an alternate modality for the treatment of primary and secondary lung cancers. This therapy has the important advantages of allowing shortened treatment times while delivering higher effective radiobiological doses. However, normal tissues surrounding the tumors are also exposed to high-dose levels of radiation. Furthermore, cancerous tissue can occasionally move outside the irradiation field, e.g. when the patient has sudden irregular breathing or episodes of coughing. Under these circumstances, malignant tissue will be missed, and even more normal tissue than planned will be irradiated. A very large fractional dose (e.g., 5 Gy or more) is commonly applied in hypofractionated lung radiotherapy. Consequently, this is in many ways an ablative therapy, both to the tumors and to the normal tissues surrounding them. Consequently, the precision requirement of hypofracionated lung radiotherapy is high. It is absolutely critical to effectively monitor the target to ensure maximal irradiation of the tumor with minimal irradiation of surrounding normal tissue.

The major uncertainty in treating lung cancer is the respiratory lung tumor motion, which can be clinically significant for some patients (e.g., of the order of 2 – 3cm) [2]. This uncertainty must be dealt with when delivering hypofractionated lung radiotherapy. Typically, margins are added to accommodate respiratory motion. However, even with margins, tumors, or portions of them, will occasionally move outside the irradiation field. Abrupt coughing, dramatically changing breathing patterns, and sudden occurrences of pain, all can occur during treatment. Any one of these events can result in part or the entire tumor moving outside the irradiation field. It is critically important to constantly monitor the patients' treatment—when the tumor is detected outside the irradiation field, the treatment must be interrupted. The treatment should be resumed only when the tumor returns to the irradiation field or, in extreme cases, after patient re-setup.

EPID acquisition in *cine* mode does not require additional radiation dose, and yet the images generated carry information indicating tumor position. Several methods for monitoring radiation therapy have been developed using *cine* EPID images, with or without implanted markers.

978-0-7695-3495-4/08 $25.00 © 2008 IEEE
DOI 10.1109/ICMLA.2008.150

Berbeco *et al.* developed a matching technique for respiratory-gated liver radiotherapy treatment verification with an EPID in *cine* mode [3, 4]. Implanted radio opaque fiducial markers inside or near the target are required for this technique. The markers are contoured on the planning CT set, enabling users to create digitally reconstructed radiographs (DRRs) for each treatment beam. During the treatment, a sequence of EPID images can be acquired without disrupting the treatment routine. Implanted markers are visualized in the images and their positions in the beam's eye view (BEV) are calculated off-line and compared to the reference position by matching the field apertures in corresponding EPID and DRR images. Tumor displacement was calculated for one patient with three implanted markers. The case study demonstrated the feasibility of the proposed method.

For lung cancer patients, implantation of fiducial markers is not widely acceptable due to the risk of pneumothorax [3, 5-8]. Arimura *et al.* considered using *cine* EPID images for measurement of displacement vectors of tumor position in lung radiotherapy without implanted markers [9]. A template matching technique based on cross-correlation coefficients was proposed to calculate the similarity between a reference portal image and each *cine* EPID image. 5 patients with non-small cell lung cancer and one patient with metastasis were included for a validation study. The proposed method worked well for 4 cases but not well for the other 2.

To develop a more robust system, we propose an alternative approach for treatment verification of hypofractionated lung radiotherapy using *cine* EPID images without implanted markers. Artificial Neural Network (ANN) based technique will be developed to classify the *cine* EPID images into two classes: images with the tumor inside the radiation field and images with the tumor outside the radiation field.

This paper is organized as follows: section 2 will introduce methods and materials used in this work, including brief introduction of ANN and detailed description of how to apply it to our treatment verification problem. Section 3 presents experimental results. Section 4 will conclude this work and plan future work.

2. Methods and materials

The goal of on-line treatment verification is to monitor the tumor to verify if it is inside the radiation field (or beam aperture). If it is inside, treatment goes on. Otherwise, treatment beam should be turned off. This provides us with a clue that the on-line treatment verification problem can in fact be modeled as a classification problem. EPID *cine* images correspond to tumor inside the aperture can be treated as one class, and EPID *cine* images correspond to tumor outside the aperture can be treated as another class. In this work, we apply a machine learning algorithm, ANN, for treatment verification. We will test its feasibility off-line retrospectively for hypofractionated lung radiotherapy.

2.1. Artificial Neural Network. An Artificial Neural Network is a mathematical model inspired by the way biological nervous system processes information. ANN includes massively parallel systems with large numbers of interconnected simple processors, and it can solve many challenging computational problems. For classification problem, ANN will learn example (training samples) of each class to extract its corresponding patterns and detect its unique trends. A trained ANN can therefore classify new samples into corresponding classes with high accuracy. More details on applying ANN on cancer research can be found in [10].

2.2. Training ANN. The first step of the ANN is learning, or training from samples. A trained neural network can be thought of as an "expert" in the category of information it has been given to analyze. In our application of hypofractionated lung radiotherapy verification using *cine* EPID images, the ideal training samples would naturally be *cine* EPID images. There are, however, two problems. First, ANN requires a large number of training samples to achieve reasonable results, and there aren't enough *cine* EPID images generated during the treatment to meet that standard. Second, to be able to verify the treatment using *cine* EPID images during the treatment, the ANN training has to be completed before the treatment, when the *cine* EPID images are not yet available. For these reasons, *cine* EPID images cannot be used as training samples.

We generate training images from DRR—to simulate *cine* EPID images with various artificially altered tumor locations. DRRs were created in the BEV for each field. The field edges (MLC contours) were superimposed on these images. The first image in Figure 1 illustrates an example of DRR of a treatment field. The solid red contour is the MLC contour. By shifting the MLC contour, the sub-image defined by the contour changes accordingly. If each sub-image is treated as a simulated *cine* EPID image, we can simulate *cine* EPID images with different tumor locations. Once again, consider the first image of Figure 1: the blue and green dashed contours are two examples of MLC contour at different locations. Tumor locations are different in the sub-images outlined by the corresponding contours. In this fashion, we can simulate *cine* EPID images with different tumor locations. The two images on the right side of Figure 1 are the

enlarged versions of the sub-images defined by the blue and green dashed contours in the first image, respectively. If we limit the MLC contour to move inside of an $m \times n$ pixel sized window at the step size of one pixel, we can generate mn training images.

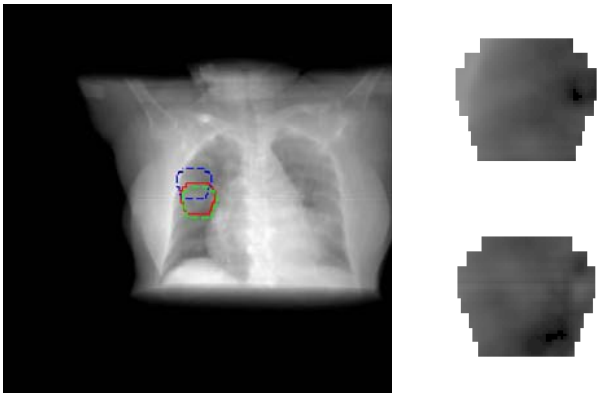

Figure 1 The image on the left: DRR of a treatment field. The solid red contour is the MLC edge. The blue and green dashed contours define two examples of the training images for ANN. The sub-images inside the blue and green contours have been enlarged and displayed on upper right and lower right, respectively.

The clinical target volume (CTV) is defined by the physician on 4DCT and is projected onto each DRR. Based on the location of the CTV, we can calculate what percentage of the tumor is in the beam aperture of each training image. With a user-defined threshold p%, we associate class 1 to the training image if more than p% of the tumor is in MLC and class -1 otherwise.

From the total of mn training images, the ANN can learn what features indicate class 1 and what features indicate class -1. It can create its own organization or representation of the information it receives during the learning time. The trained network can therefore analyze the *cine* EPID images obtained during the treatment and classify them into the corresponding class 1 or -1.

2.3. Image processing. As we stated above, we used DRR instead of *cine* EPID images for neural network training. However, DRR and *cine* EPID images are different image modalities. Their pixel resolutions might be different, and their intensity values might be in different ranges. To enhance the ANN's performance, we applied image processing techniques to the DRR to make DRR and *cine* EPID images more closely resemble each other. First we either sub-sample or interpolate DRR to make its resolution the same as *cine* EPID image, depending on the original resolution of DRR. Then, histogram equalization was applied on each DRR and *cine* EPID image to enhance image contrast. Finally, the intensity value of DRR was mapped to the same range of *cine* EPID images. Based on our experience, pre-processing the images can significantly improve the ANN performance.

2.4. Principal Component Analysis (PCA). A typical *cine* EPID image might have an approximate size of 100×100 pixels. This means the dimensionality of a training sample would be $100 \times 100 = 10,000$. Significant computational time and resources would be needed to train the ANN with these high dimensional samples. This is simply not practical for on-line treatment verification. Consequently, PCA was applied to reduce the dimensionality of the training images. PCA is a classical statistical method. It involves a mathematical procedure that transforms original correlated variables into a small number of uncorrelated variables called principal components. The first principal component accounts for as much of the variability in the data as possible, and each succeeding component accounts for as much of the remaining variability as possible. In our application, we keep the first 15 principal components. Training 451 images with a reduced dimensionality of 15 using an un-optimized Matlab program on a regular PC (Intel Xeon CPU with 2 GB RAM) resulted in a running time of less than 3 seconds, demonstrating the effectiveness of this refinement.

3. Experimental results

In our clinic, all hypofractionated lung radiotherapy patients are treated on a Varian Trilogy linac (Varian Medical Systems, Palo Alto, CA, USA) equipped with an electronic portal imaging device. During the treatment, the EPID was set to acquire images in the *cine* mode at a frame rate of 0.625 Hz. Figure 2 shows two sample *cine* EPID images. The corresponding DRR was shown in Figure 1.

Figure 2 Examples of *cine* EPID images.

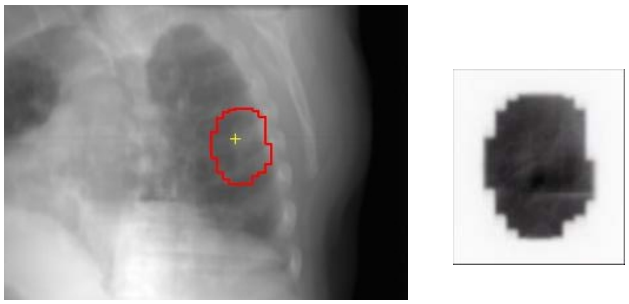

Figure 3 DRR and *cine* EPID image.

Six patients each treated with 4 or 5 fractions were included for our feasibility study. The total number of *cine* EPID images of each patient varies from 84 to 329 depending on the treatment time. The examples of DRR and *cine* EPID images of patient 1 were displayed in Figure 1 and Figure 2. Figure 3 shows examples of DRR and *cine* EPID image of patient 2. The red contour on the DRR defines the bean aperture. Window size of 40×10 pixels was used on each DRR to generate the training images. A radiation oncologist read the *cine* EPID images and manually classified them into classes 1 and -1, and this serves as our ground truth. The ANN was applied on the training images to build the neural network. We set in this study—if more than 95% of the tumor is inside the irradiation field, the corresponding training image is said in class 1. For each treatment field, one neural network needs to be built.

We measure the accuracy, recall and precision of the classification results. They are defined as:

$$\text{recall} = \frac{\text{true positive}}{\text{true positive} + \text{false negative}} \quad (1)$$

$$\text{precision} = \frac{\text{true positive}}{\text{true positive} + \text{false positive}} \quad (2)$$

$$\text{accuracy} = \frac{\text{true positive} + \text{true negative}}{\text{all}} \quad (3)$$

Accuracy measures the degree of exactness or fidelity, recall measures the degree of completeness, and precision measures the degree of reproducibility.

Patient	Accuracy	Precision	Recall
1	94.12	100.00	94.12
2	99.87	98.86	98.89
3	97.00	100.00	97.00
4	98.86	99.87	98.89
5	98.91	100.00	98.91
6	79.17	100.00	79.17
Average	**94.66**	**99.79**	**94.50**

Table 1 Classification results in percentage.

Table 1 lists the classification results of all six patients. Each number was averaged over all treatment fields. The average accuracy, precision, and recall numbers over all the patients are also listed in the last row of the table.

The accuracy and recall results of patient 6 are low, although the precision of patient 6 is 100 percent. For all other patients, the results are good; the numbers are in high nineties most of the time. Note all the precisions are either 100% or close to 100%. This means the reproducibility is high, and the proposed algorithm is stable. On average, the proposed algorithm achieved accuracy of 94.66%, precision of 99.79%, and recall of 94.50%.

4. Conclusion and future work

We have proposed a novel approach for on-line treatment verification for hypofractionated radiotherapy. DRR was used to simulate *cine* EPID images for ANN training. Image processing techniques were applied on DRR to make DRR and *cine* EPID images closely resemble each other. PCA was also applied on training samples and *cine* EPID images acquired during the treatment to reduce their dimensionality in order to shorten the process time. We have tested our proposed algorithm on six hypofractioned lung patients off-line in a retrospective fashion. The average accuracy and recall numbers are high, and the average reproducibility is close to 100%.

We intend to achieve even better results. More sophisticated image processing techniques will be applied to preprocess the DRR. We have already experienced a significant performance boost from pre-processing the images with the techniques described. Better image processing techniques should bring the classification accuracy rate even higher. All the ANN parameters were not optimized. We will investigate different combinations of parameters to find the set that yields the best performance. Now we use kV beam DRR. We are developing software to generate MV beam DRR with scattering effect which will better resemble *cine* EPID images obtained during the treatment. We are also collecting more patient data, hopefully with implanted fiducial markers, to further validate our proposed algorithm.

5. References

[1] A. Jemal, T. Murray, E. Ward, A. Samuels, R. C. Tiwari, A. Ghafoor, E. J. Feuer, and M. J. Thun, "Cancer statistics," *CA Cancer J. Clin.,* vol. 55, pp. 10-30, 2005.

[2] S. B. Jiang, "Radiotherapy of mobile tumors," *Semin Radiat. Oncol.,* vol. 16, pp. 239-48, 2006.

[3] R. I. Berbeco, H. Mostafavi, G. C. Sharp, and S. B. Jiang, "Towards fluoroscopic respiratory gating for lung tumours without radiopaque markers," *Int. of Phys. Pub.,* vol. 50, pp. 4481-90, 2005.

[4] R. I. Berbeco, F. Hacker, D. Ionascu, and H. J. Mamon, "Clinical feasibility of using an EPID in *cine* mode for image-guided verification of stereotactic body radiotherapy," *Int. J. Radiation Oncology Biol. Phys.,* vol. 69, pp. 258-266, 2007.

[5] F. Laurent, V. Latrabe, B. Vergier, M. Montaudon, J. M. Vernejoux, and J. Dubrez, "CT-guided transthoracic needle biopsy of pulmonary nodules smaller than 20 mm: results with an automated 20-gauge coaxial cutting needle," *Clin. Radiol.,* vol. 55, pp. 281-7, 2000.

[6] S. Arslan, A. Yilmaz, B. Bayramqurler, O. Uzman, E. Nver, and E. Akkaya, "CT-guided transthoracic fine needle aspiration of pulmonary lesions: accuracy and complications in 294 patients," *Med. Sci. Monit.,* vol. 8, pp. CR493-7, 2002.

[7] P. R. Geraghty, S. T. Kee, G. McFarlane, M. K. Razavi, D. Y. Sze, and M. D. Dake, "CT-guided transthoracic needle aspiration biopsy of pulmonary nodules: needle size and pneumothorax rate," *Radiology,* vol. 229, pp. 475-81, 2003.

[8] U. Topal and B. Ediz, "Transthoracic needle biopsy: factors effecting risk of pneumothorax," *Eur. J. Radiol.,* vol. 48, pp. 263-7, 2003.

[9] H. Arimura, S. Anai, S. Yoshidome, K. Nakamura, Y. Shioyama, S. Nomoto, H. Honda, Y. Onizuka, and H. Terashima, "Computerized method for measurement of displacement vectors of target positions on EPID *cine* images in stereotactic radiotherapy," in *Medical Imaging*. vol. 6512: Proc. of SPIE, 2007.

[10] R. N. Naquib and G. V. Sherbet, *Artificial neural networks in cancer diagnosis, prognosis, and patient management*: CRC Press, 2001.